
# *Late Pleistocene and possibly Holocene displacement along the Rendija Canyon Fault, Los Alamos County, New Mexico*

Keith I. Kelson, Mark Hemphill-Haley, Susan S. Olig, Simpson, Gary, D., Jamie N. Gardner, Steven L. Reneau, Thomas R. Kolbe, Steven L. Forman, and Ivan G. Wong, 1996, pp. 153-160

*in:*

*Jemez Mountains Region*, Goff, F.; Kues, B. S.; Rogers, M. A.; McFadden, L. S.; Gardner, J. N.; [eds.], New Mexico Geological Society 47th Annual Fall Field Conference Guidebook, 484 p.

*This page is intentionally left blank to maintain order of facing pages.*

# LATE PLEISTOCENE AND POSSIBLY HOLOCENE DISPLACEMENT ALONG THE RENDIJA CANYON FAULT, LOS ALAMOS COUNTY, NEW MEXICO

KEITH I. KELSON[1], MARK A. HEMPHILL-HALEY[2], SUSAN S. OLIG[3], GARY D. SIMPSON[1], JAMIE N. GARDNER[4], STEVEN L. RENEAU[4], THOMAS R. KOLBE[3], STEVEN L. FORMAN[5] and IVAN G. WONG[3]

[1]William Lettis & Associates, Inc., Walnut Creek , CA 94596; [2]University of Oregon, Department of Geological Sciences, Eugene, OR 97403; [3]Woodward-Clyde Federal Services, Oakland CA 94607; [4]Geology and Geochemistry Group, Los Alamos National Laboratory, Los Alamos, NM 87545; [5]Byrd Polar Research Center, Ohio State University, Columbus, OH 43210

**Abstract**—The Rendija Canyon fault is an integral part of the Pajarito fault system, which forms the active western margin of the Española Basin in the Rio Grande rift. As part of a paleoseismic study, we excavated two exploratory trenches across the central part of the fault. These trenches exposed faulted alluvium overlain by two packages of scarp-derived colluvial deposits that resulted from degradation of a scarp produced by west-down normal displacement on the Rendija Canyon fault. Each colluvial package contains a lower, discontinuous debris facies close to the fault, and an upper, fine-grained wash facies. Ages of the alluvial and colluvial deposits are estimated from radiocarbon and luminescence analyses, and relative soil development. The trench exposures provided evidence of at least three and possibly as many as five surface-faulting events, with the oldest of these occurring prior to about 140 ka. Three or four events occurred since deposition of a colluvium that is more than 140 ± 26 ka. The most recent rupture occurred at about 9 or 23 ka, indicating a latest Pleistocene or early Holocene event along the fault. The thickness of the upper colluvial package suggests 2.0 ± 0.5 m of vertical displacement during the most recent paleoearthquake. We estimate an average recurrence interval for surface-rupture earthquakes of between 33 and 66 ka from age estimates of scarp-derived colluvium, and an interval of about 38 to 83 ka from long-term slip rate and displacement-per-event data. The timing of the most recent earthquake on the Rendija Canyon fault suggests that it may rupture independently from the nearby Guaje Mountain fault, which has also been active during the Holocene.

## INTRODUCTION

The Rendija Canyon fault is a west-down fault within the Pajarito fault system, which defines the western margin of the modern Rio Grande rift in northern New Mexico (Fig. 1). The Pajarito fault system is a 41-km-long series of north-striking faults that defines the western boundary of the Española Basin (Gardner and House, 1987). The primary fault within this system is the Pajarito fault (PAF), which has as much as 154 m of east-down displacement since deposition of the 1.2-Ma upper Bandelier Tuff (Olig et al., this volume). Other major faults within the Pajarito fault system include the Rendija Canyon (RCF) and Guaje Mountain (GMF) faults, which have as much as 36 m and 27 m of post-1.2 Ma displacement, respectively. In contrast to the PAF, both the RCF and GMF exhibit west-down displacement, suggesting that they are antithetic to the primary east-down, rift-bordering PAF. At their northern ends, the RCF and GMF intersect the northern part of the PAF (Fig. 2). These three faults collectively accommodate the east-west component of extension of the Española Basin. However, as components of the complex northern part of the Pajarito fault system, the RCF and GMF may reflect distributed deformation related to transfer of strain between the Española Basin and the San Luis Basin to the northeast (Fig. 1). These basins both have east-west Quaternary extension at rates of about 0.1 mm/yr (Kelson and Olig, 1995).

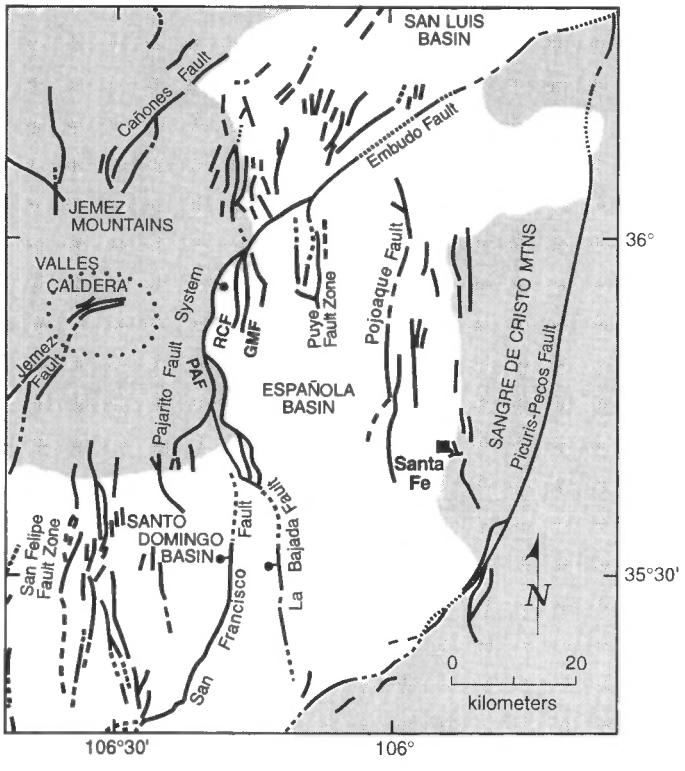


FIGURE 1. Regional tectonic map of the Española Basin, showing rift basins (unshaded) and adjacent uplifts (shaded). PAF = Pajarito fault; RCF = Rendija Canyon fault; GMF = Guaje Mountain fault.

Our investigation of the RCF was part of a seismic hazard evaluation of Los Alamos National Laboratory (LANL) (Wong et al., this volume; Olig et al., this volume), which included collection of data on the Quaternary characteristics of the Pajarito fault system. Prior to this investigation, the paleoseismic characteristics of the PAF and RCF were poorly known, although Gardner et al. (1990) show that the GMF has had repeated late Quaternary earthquakes, including a surface-faulting event about 4 to 6 ka. These data, as well as a prominent topographic escarpment along the Pajarito fault, show that the major components of the Pajarito fault system are potential seismogenic sources that pose a hazard to the western Española Basin. Wong et al. (unpubl. report for LANL, 1995) suggest a maximum moment magnitude of M6.9 for the PAF, M6.5 for the RCF, and M6.5 for the GMF. The primary goals of our studies of the RCF were to assess the timing of late Quaternary surface ruptures on the fault, and estimate the fault slip rate and recurrence interval of large-magnitude earthquakes for a probabilistic seismic hazard analysis of strong ground motion (Wong et al., this volume). Our focus here is on the paleoseismologic characteristics of the fault derived from exploratory trenching along the central part of the fault, at the Guaje Pines site (Fig. 2).

## GEOLOGIC SETTING

The 14-km-long RCF is subparallel to and approximately 3 km east of the PAF (Gardner and House, 1987), and its northern end intersects the PAF about 3 km north of the town of Los Alamos (Fig. 2). The RCF consists of a single strand north of Barranca Mesa, of two primary strands and numerous secondary strands through the town of Los Alamos, and of a zone of distributed deformation south of Los Alamos Canyon (Fig. 2). Topographic profiles show that scarps developed in the 1.2 Ma upper Bandelier Tuff are highest in the central part of the fault, with a maximum net vertical tectonic displacement of 36 ± 10 m (Fig. 3; Olig et al., this volume). The average vertical displacement along the fault is 22 m,

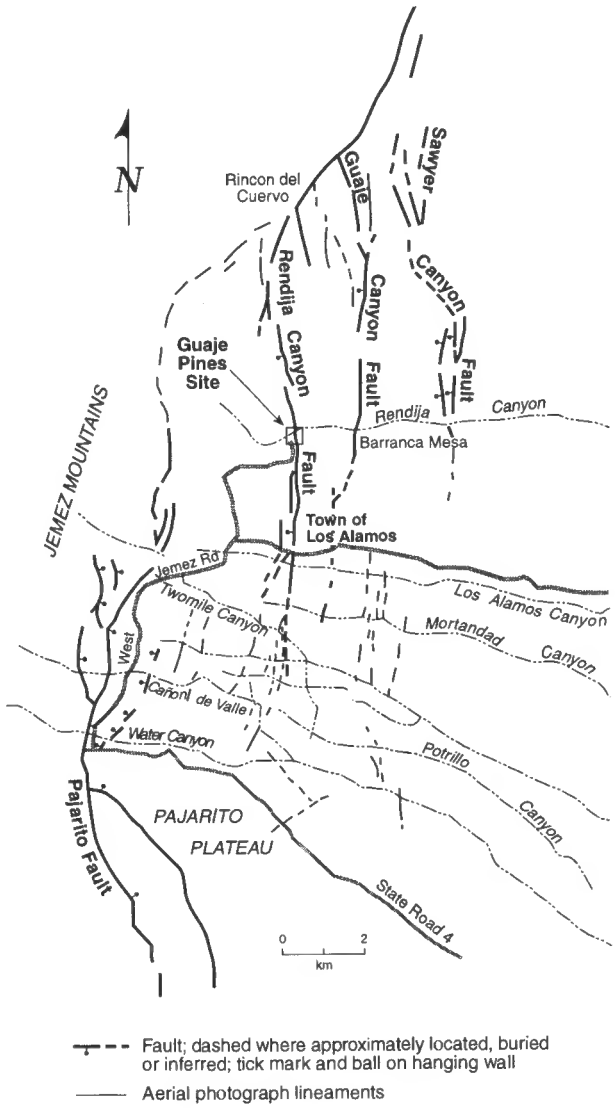


FIGURE 2. Map of the northern Pajarito Plateau, showing major fault traces within the Pajarito fault system.

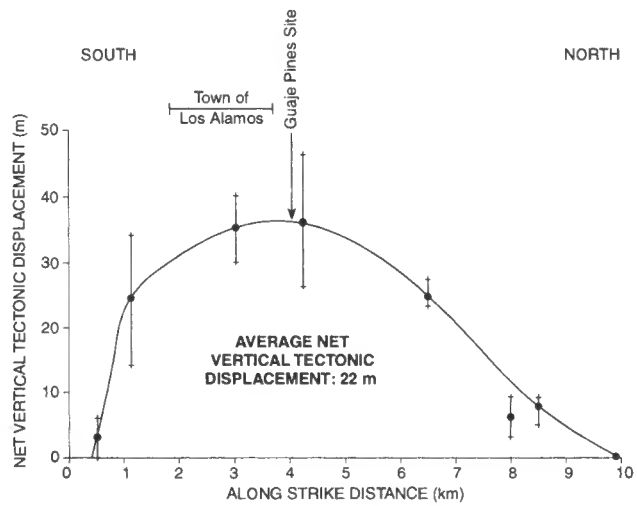


FIGURE 3. Apparent net vertical tectonic displacement of the 1.2 Ma upper Bandelier Tuff along the Rendija Canyon fault. We assume that the apparent displacements of the topographic surface underlain by the tuff approximate the net vertical tectonic displacements across the fault.

which yields an average minimum long-term vertical slip rate of 0.02 mm/yr, assuming the observed vertical displacement occurred continuously since 1.2 Ma. The vertical slip rate based on 36 ± 10 m of displacement is 0.03 ± 0.01 mm/yr. Carter and Gardner (1995) stated that slickenside lineations are steeply plunging to near-vertical along the fault, and use kinematic analysis of these data to interpret that the axis of least principal horizontal stress (i.e., extension) trends approximately east.

We selected the Guaje Pines site on the central part of the fault for detailed paleoseismic investigations because there is a prominent, west-facing topographic scarp across late Quaternary alluvial deposits (Fig. 4). The fault scarp is along the western side of a small hill composed of Miocene-Pliocene dacites of the Tschicoma Formation (Smith et al., 1970), which is overlain by older alluvium deposited by the ancestral Rendija Canyon drainage. Notably, the scarp opposes the east-flowing drainages in the site area. On the downthrown (western) side of the scarp, scarp-derived colluvial deposits overlie sediments associated with a broad, gently east-sloping alluvial surface. Our investigations included excavation of four trenches; two trenches across the scarp (GPT1 and GPT2, Fig. 4) to expose stratigraphic units and fault-related features, and thus to obtain data on the number and timing of past surface faulting earthquakes; and two trenches parallel to the scarp (GPT3 and GPT4, Fig. 4) to provide a three-dimensional perspective on the stratigraphy. In addition, three soil pits were excavated to provide information on soil characteristics developed on the younger alluvial surface (SP1, SP2, and SP3, Fig. 4).

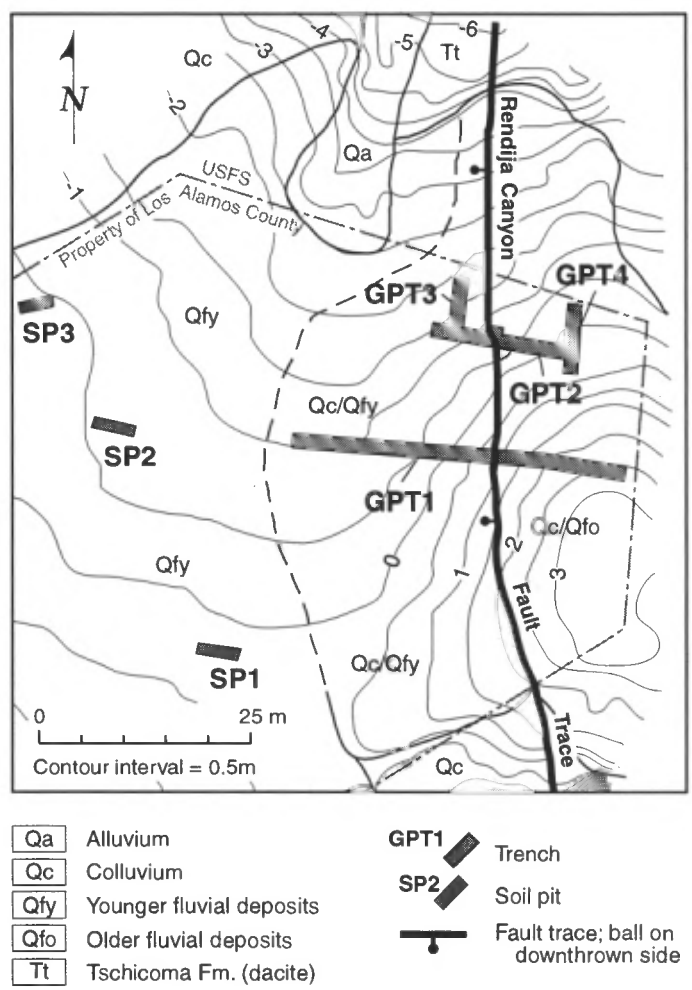


FIGURE 4. Surficial geologic map of the Guaje Pines trench site along the Rendija Canyon fault.

## STRATIGRAPHY AND STRUCTURE

### Surficial stratigraphy

The surficial stratigraphy exposed in trenches at the Guaje Pines site consists of older alluvium deposited by an ancestral east-flowing Rendija Canyon drainage (including a possible sag-pond deposit), overlain by two packages of scarp-derived colluvium. Each of these colluvial deposits contains a lower, discontinuous proximal coarse facies close to the fault, as well as an upper, finer-grained and more extensive wash facies (Fig. 5). Soil development and numerical age estimates suggest middle to late Pleistocene deposition of all of these units, with the exception of a latest Pleistocene to early Holocene age for the uppermost scarp-derived colluvium.

In general, stratigraphic relations are similar among all trenches, and correlations are straightforward on the basis of grain size, sorting, bedding thickness and continuity, and relative soil development. The differentiation between alluvium and scarp-derived colluvium is based on variations in grain size within each trench exposure. Alluvial beds typically are well sorted and contain clasts of consistent size, whereas the colluvial deposits typically are coarser and poorly sorted adjacent to the fault and finer to the west, away from the fault. Four observations support our interpretation that the colluvial deposits are related to degradation of a scarp produced during a paleoearthquake: (1) the presence of the colluvium only on the downthrown side of the fault scarp; (2) the deposits decrease in thickness away from the fault scarp and are wedge-shaped in cross section; (3) the percentages and sizes of clasts progressively decrease to the west, away from the fault; and (4) their association with deposits that appear to have filled fissures along the fault trace. These are all characteristics typical of colluvial deposits derived from fault scarps (Nelson, 1992). Figures 6 and 7 provide detailed maps of the walls of the two cross-fault trenches, and show stratigraphic and structural relations adjacent to the fault.

### Older alluvial deposits

The oldest surficial deposits exposed in the trenches at the Guaje Pines site are two alluvial units overlying dacite bedrock on the upthrown side of the fault (units A1 and A2, Fig. 7). The lowest of these, a fluvial clayey gravel in trench GPT2 (unit A1), has a pebble bed resting on the bedrock surface. Because this bed and the bedrock surface dip about 20° west, it is likely that these deposits have been tilted to the west during one or more large earthquakes. Overlying unit A1 is a massive, olive gray sandy clay that contains prismatic soil structure and pedogenic clay films (unit A2, Fig. 7). This soil is subhorizontal and suggests that the tilting that deformed unit A1 preceded the deposition of unit A2. Unit A2, which is faulted against younger alluvium at its western end, is interpreted as a quiet-water (sag-pond?) deposit that may be related to surficial deformation along the RCF. The age of unit A2 is based on one thermoluminescence (TL) analysis of silt (GPT2-TL5, Fig. 7), which yielded an age estimate of >140 ± 26 ka (Table 1).

A package of relatively well-bedded, oxidized alluvial deposits unconformably overlies units A1 and A2 (unit A3, Figs. 6, 7). These deposits, which are identified only east of the fault, have distinctive bedding and oxidation, and likely were derived from an ancestral Rendija Canyon drainage. These may correlate with the middle Pleistocene Qt1 or Qt2 deposits mapped by Wong et al. (unpubl. report for LANL, 1995) and McDonald et al. (this volume). The lack of evidence of near-surface soil horizons within the deposits suggests that the upper part of the unit is eroded. The western part of unit A3 is faulted against younger deposits west of the fault, but it is not cut by a fault splay in trench GPT2 that displaces the underlying unit A2 between stations 6 and 9 m (Fig. 7). The age of unit A3, which is constrained by TL analyses from overlying deposits, is more than about 65 ka (see below).

On the western (downthrown) side of the fault, the oldest deposit exposed is a boulder gravel deposited by the Rendija Canyon drainage (unit

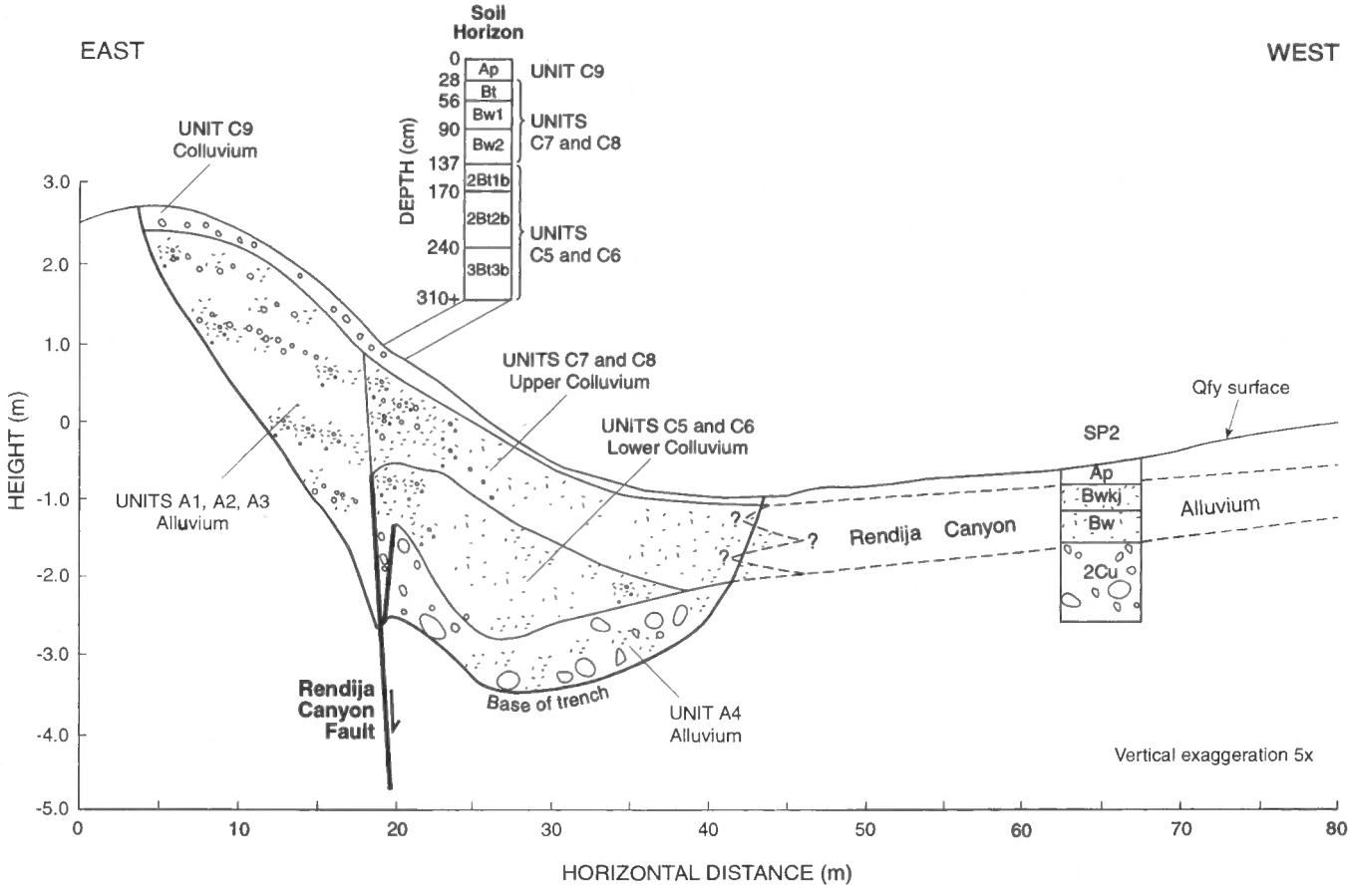


FIGURE 5. Schematic cross section across the Rendija Canyon fault at the Guaje Pines site, showing generalized stratigraphic and structural relations exposed in trenches GPT1 and GPT2, and soil pit SP2.

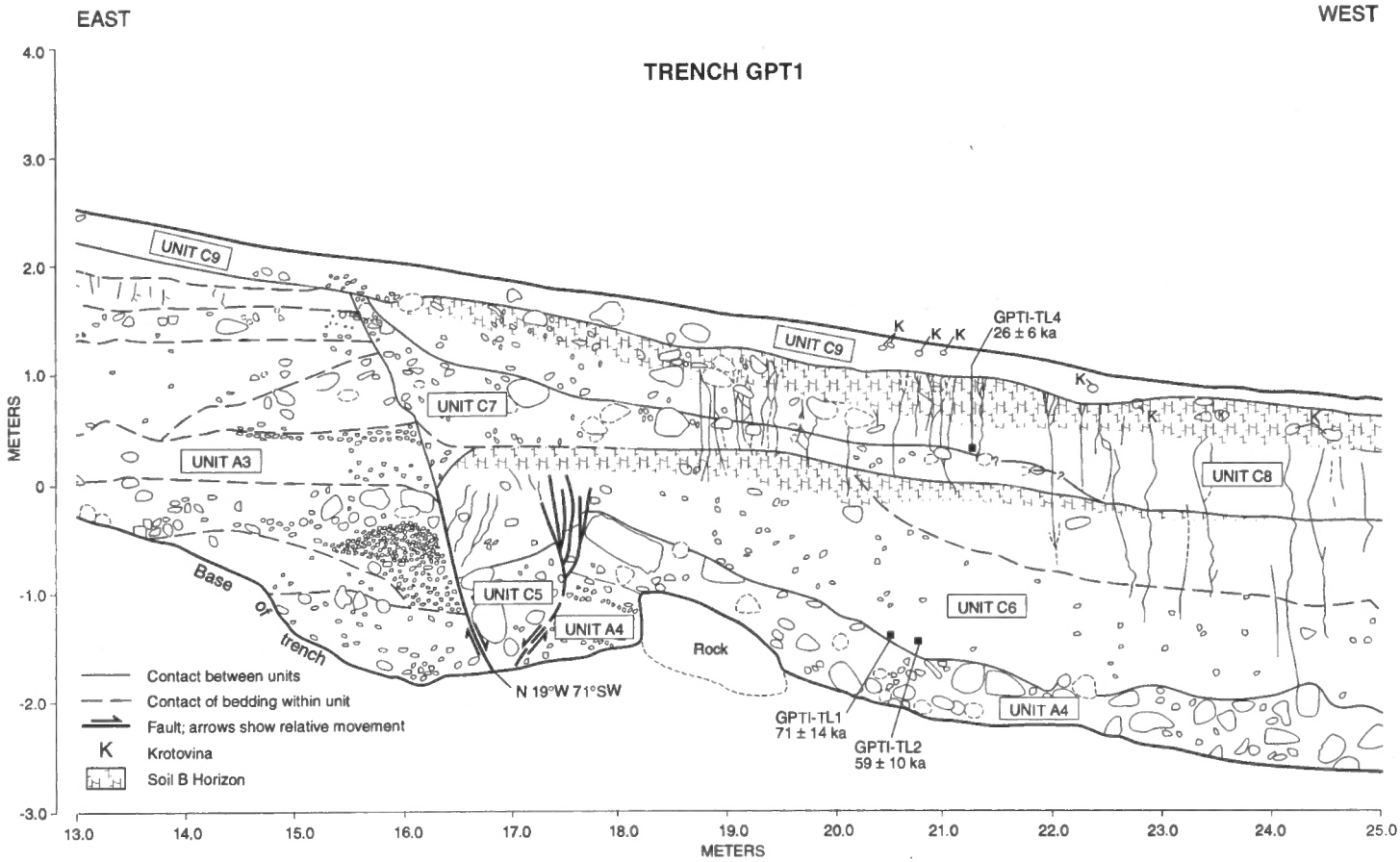


FIGURE 6. Log of the Rendija Canyon fault exposed in trench GPT1.

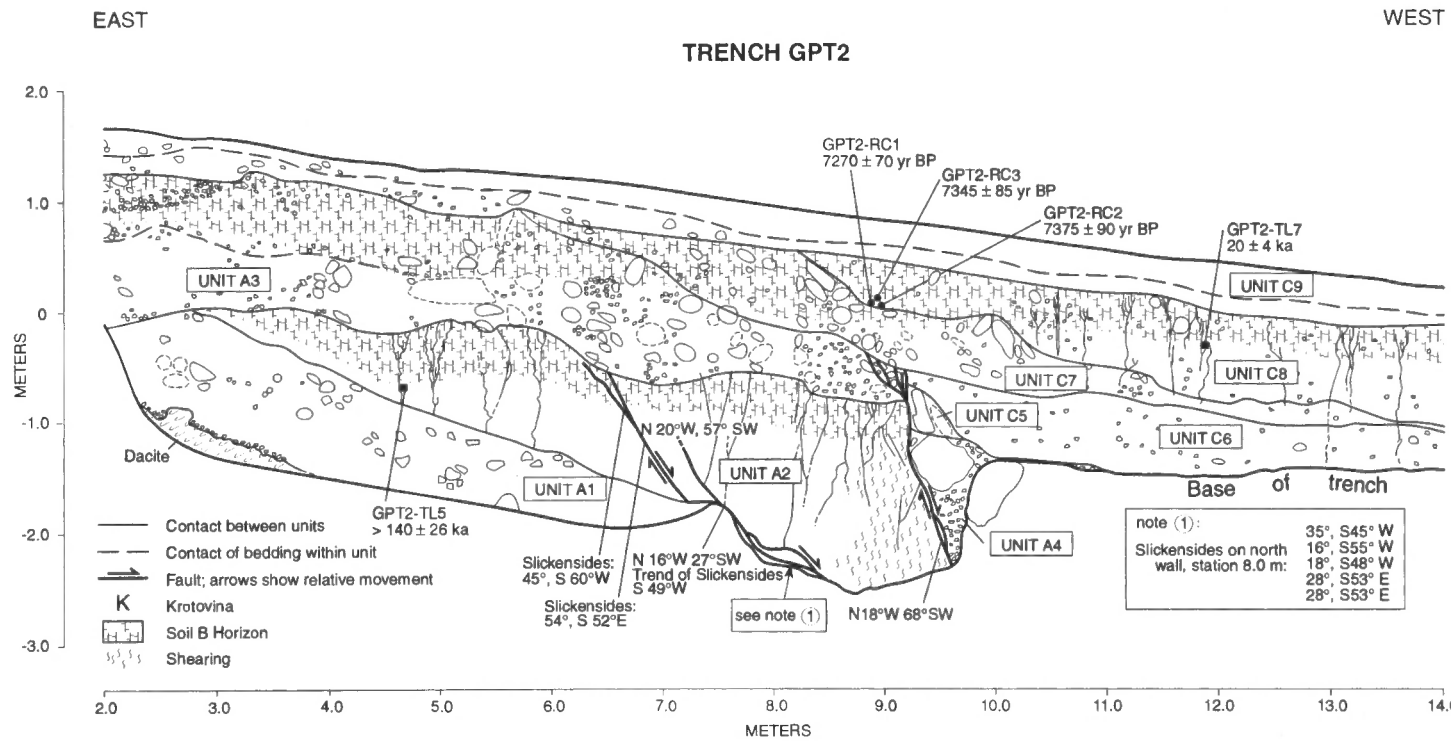


FIGURE 7. Log of the Rendija Canyon fault exposed in trench GPT2.

TABLE 1. Thermoluminescence samples and analyses from the Guaje Pines site.

| Geologic unit | Field number | Lab number | Equivalent dose method† | Light exposure (hours)@ | Temperature range or time# | Equivalent dose (grays)‡ | TL age estimate (ka)* |
|---|---|---|---|---|---|---|---|
| C8 | GPT2-TL7 | OTL-478 | TB | 16 sun | 280-400°C | 79.09 ± 2.63 | 15 ± 3 |
| | | | TB | 8 UV | 280-400°C | 106.70 ± 2.08 | **20 ± 4** |
| | | | PB | 1 sun | 280-400°C | 109.10 ± 3.07 | 21 ± 4 |
| C8 | GPT1-TL4 | OTL-519 | TB | 16 sun | 250-400°C | 108.70 ± 2.35 | 24 ± 6 |
| | | | TB | 8 UV | 250-400°C | 118.60 ± 1.43 | **26 ± 6** |
| | | | OSL-IR | 1 sun | 3 to 59 sec | 113.20 ± 1.27 | 26 ± 6 |
| C8 | | | | | | Average of preferred values: | **23± 4** |
| C6 | GPT1-TL2 | OTL-463 | TB | 16 sun | 300-390°C | 338.10 ± 6.76 | **59 ± 10** |
| | | | PB | 1 sun | 300-390°C | 337.6 ± 214.7 | 58 ± 52 |
| C6 | GPT1-TL1 | OTL-518 | TB | 16 sun | 260-360°C | 385.4 ± 6.82 | **71 ± 14** |
| | | | OSL-IR | 1 sun | 2 to 23 sec | 383.97 ± 6.99 | 69 ± 14 |
| C6 | | | | | | Average of preferred values: | **65 ± 9** |
| A2 | GPT2-TL5 | OTL-477 | TB | 16 sun | 290-400°C | 2026.9 ± 126.4 | **>140 ± 26** |

† All TL measurements made with a Corning 5/58, and HA-3 filters in front of the photomultiplier tube. Samples were preheated to 124°C for 48 hours prior to analysis. TB = total bleach; PB = partial bleach; OSL-IR = optically stimulated luminescence with infrared radiation.

@ Hours of light exposure to define residual level. "Sun" is natural sunlight in Columbus, Ohio. UV is light exposure from 275 watt General Electric "sunlamp".

# Temperature range used to calculate equivalent dose; time used for OSL samples.

‡ For equivalent dose, all error limits are one sigma and are calculated by averaging errors across the temperature range.

* Preferred age estimates in **bold**, with error limits of two sigma. Moisture content of 15 ± 5% assumed for age calculations.

A4, Figs. 6, 7). This unit was poorly exposed because it contains large (1.5 m diameter) dacite boulders that precluded deep excavation of trenches GPT1 and GPT2. Adjacent to the fault in trench GPT1, unit A4 dips to the west as a result of deformation along the fault.

**Lower scarp-derived colluvial deposits**

Overlying unit A4 are two units that together comprise a colluvial sequence that is finer grained upward and westward, away from the fault (units C5 and C6, Figs. 5-7). Unit C5 is present only adjacent to the fault, and consists of coarse gravel with dacite clasts as much as 0.5 m in diameter. This unit is interpreted as the proximal facies of scarp-derived colluvium deposited shortly after a surface-rupture earthquake. The source of these deposits appears to be the coarse gravel of unit A3 that was exposed in a scarp face during a surface rupture. Within the fault zone in trench GPT1, unit C5 appears to fill a small graben or is a tectonically mixed zone of unit A4 (Fig. 6). This debris colluvium grades upward into unit C6, which contains gravel clasts that are smaller and less abundant than in unit C5. This deposit is interpreted as a scarp-derived wash colluvium deposited hundreds to perhaps a few thousand years after a surface-rupture earthquake. Both units C5 and C6 are displaced by the RCF (Figs. 6, 7). The age of unit C6 is estimated on the basis of two TL analyses on silt from the base of the deposit (GPT1-TL1 and GPT1-TL2, Fig. 6). These analyses yielded age estimates of about 71 and 59 ka, respectively, which have a root-mean square average of 65 ± 9 ka (Table 1).

Remnants of a prominent soil horizon are preserved in the upper part of unit C6 in trench GPT1 (Fig. 6). The upper 33 cm of this buried soil has secondary clay accumulation, medium subangular blocky structure, reddening (7.5YR hues), and clay films (horizon 2Bt1b, Fig. 5); all of which are indicators of an argillic B horizon. The total thickness of the buried B horizons developed in unit C6 is 103 cm, which in conjunction with the amount of clay accumulation, suggests several tens of thousands of years of soil formation.

**Upper scarp-derived colluvial deposits**

Directly overlying unit C6 in both trenches is a second package of scarp-derived colluvium (units C7 and C8, Figs. 6, 7). These units also are a fining-upward sequence of gravel, silty gravel, and silt that in general contains smaller and fewer clasts to the west, away from the fault. Directly adjacent to the fault in trench GPT1, the basal part of unit C7 contains a gravelly silt that appears to have been deposited in a depression or small fissure along the fault trace (Fig. 6). Based on clast sizes and stratigraphic position, unit C7 probably was derived from unit A3 exposed in a scarp face shortly following a surface-faulting earthquake. Unit C8 probably also was derived from the scarp produced during this earthquake, although the westernmost (distal) parts of this unit may also contain some windblown material and interbeds of fluvial gravel and silt derived from the Rendija Canyon drainage (Fig. 5). We interpret unit C7 as proximal scarp-derived colluvium, and unit C8 as a wash colluvium derived from the Rendija Canyon fault scarp.

The uppermost part of unit C8 has evidence of soil formation, including a moderately developed, 28-cm-thick Bt horizon, secondary clay accumulation, angular blocky structure, reddening (7.5YR hues), and clay films (Wong et al., unpubl. report for LANL, 1995). The Bt horizon overlies additional Bw horizons that have only minor soil development. The soil extends to the east in trench GPT2, where it is present in unit A3 on the upthrown side of the fault (Fig. 7). This soil probably took several thousand years to develop.

The ages of units C7 and C8 are based on three radiometric analyses of charcoal and two TL analyses of silt (Fig. 6; Wong et al., unpubl. report for LANL, 1995). Unfortunately, these analyses provide conflicting results and make estimation of the ages of units C7 and C8 equivocal. Radiometric analyses of three charcoal samples from the basal part of unit C8 in trench GPT1 yielded age ranges of 8000 to 8130 cal. yr BP, and an average age of 8100 ± 200 cal. yr BP (Table 2). There is no reason to suspect that these samples were contaminated or stratigraphically out of context. In contrast, two TL analyses performed on sediment from the basal part of unit C8 yielded age estimates of 20 to 26 ka (Table 1). The average of these estimates is 23 ± 4 ka, which is significantly older than the age estimate based on radiocarbon analyses. These TL samples were from different trenches, showed no evidence of anomalous fading, have small laboratory errors, and have no statistical differences in age for split samples analyzed by both the total-bleach and partial-bleach methods (Wong et al., unpubl. report for LANL, 1995). Thus, we find no reason to suspect the validity of the TL age estimates. These numerical age estimates suggest that the basal part of unit C8 is either about 8 ka (assum-

TABLE 2. Radiocarbon samples and analyses from the Guaje Pines site.

| Geologic unit | Field Number | Laboratory numbers† | Radiocarbon age (yr BP)@ | Calibrated age (cal. yr BP)# |
|---|---|---|---|---|
| C8 | GPT2-RC1 | Beta-55320 CAMS-3719 | 7270 ± 70 | 8000-8060 [7767-8335] |
| C8 | GPT2-RC2 | Beta-59678 ETH-10052 | 7375± 90 | 8130 [7800-8484] |
| C8 | GPT2-RC3 | Beta-59675 ETH-10058 | 7345 ± 85 | 8120 [7792-8414] |
| C8 | | Average‡: | 7321 ± 94 | 8030-8110 [7918-8319] |

† All analyses used accelerator mass spectrometry (AMS) methods.
@ Radiocarbon ages corrected for $^{13}C$ in laboratory; lab error limts are one sigma.
# Calibrated using CALIB 3.0 (Stuiver and Reimer, 1993), with error multiplier of 2.0 and 2-sigma uncertainty [in brackets]. Age range given for samples with several intercepts.
‡ Average ages from CALIB 3.0, with error multiplier of 2.0 for original analyses.

ing that the radiocarbon analyses are valid), or about 23 ka (assuming that the TL analyses are valid).

The age estimates for the basal part of unit C8 show that the deposition of unit C7 occurred prior to either 8 ka or 23 ka. Because this proximal colluvium probably was deposited relatively rapidly as a result of fault-scarp degradation, and because of an absence of soil development, it is likely that unit C7 is at most about one thousand years older than unit C8. Thus, we interpret that unit C7 was deposited shortly after a surface-rupture earthquake, at either approximately 9 ka or 23 ± 4 ka.

The uppermost deposit exposed in trenches at the Guaje Pines site is unit C9, an unfaulted silty colluvium that contains reworked prehistoric and historic artifacts (Figs. 6, 7). This colluvium is being transported by active slope processes, and may be a result of accelerated transport down the scarp following the initial clearing of pine trees and cultivation of the area in the early 1900s.

### Structure

The main strand of the RCF, as exposed in trenches GPT1 and GPT2, dips about 70° to the southwest, and strikes about N20°W (Figs. 6, 7). A subsidiary strand exposed in trench GPT2 has a shallow to moderate dip (27° to 57°SW) and also strikes about N20°W (Fig. 7). We encountered no slickensides along the main fault strand in the sheared surficial deposits. Trench GPT1 exposed a main, west-dipping fault, as well as an east-dipping antithetic fault (Fig. 6). These faults form a small, 1-m-wide graben that is filled with the lower proximal debris colluvium (unit C5). Structurally higher along the main strand in this trench is a small fissure fill less than 40 cm wide at the base of the upper proximal debris colluvium (unit C7, Fig. 6). In contrast, trench GPT2 contained no evidence of graben or fissure formation; the fault is expressed as a single strand (Fig. 7). This indicates minor along-strike variations in the style of faulting between the trenches, which are only about 13 m apart (Fig. 4).

## PALEOSEISMIC EVIDENCE OF LATE QUATERNARY FAULTING

Stratigraphic and structural relations exposed in trenches GPT1 and GPT2 at the Guaje Pines site provide evidence of at least three and possibly five surface-rupture earthquakes along the RCF. The trench exposures also yielded some information that helps assess the average time interval between surface ruptures, as well as the possible range in displacement that occurred during these events. This information is needed for characterizing the RCF as a potential seismic source, and thus is critical in assessing seismic hazards at LANL (Wong et al., this volume). The following section provides our interpretation of the number, timing, amount of displacement, and recurrence of late Quaternary surface ruptures of the RCF at the Guaje Pines site.

### Number and timing of paleoearthquakes

We interpret the occurrence of at least one paleoearthquake between the deposition of units A1 and A2, and probably three and possibly four

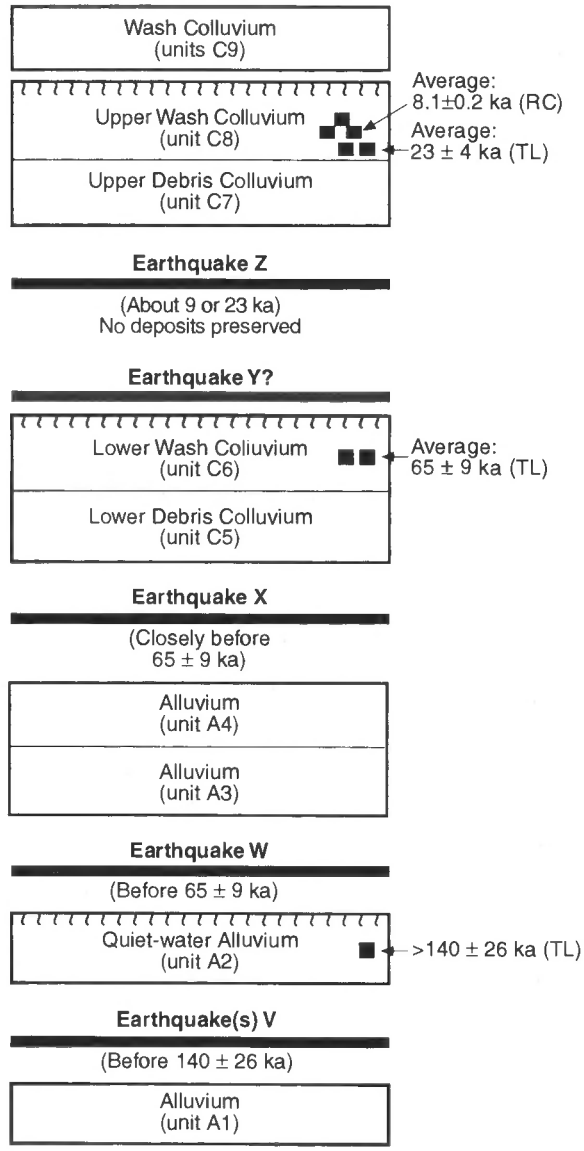


FIGURE 8. Sequence of depositional and surface-faulting events on the Rendija Canyon fault interpreted from trenches GPT1 and GPT2 at the Guaje Pines site. Hachures at top of selected boxes indicate presence of soil development.

surface-faulting paleoearthquakes since deposition of unit A2 (Fig. 8). The oldest of these rupture events (Earthquake(s) V, Fig. 8) is identified on the basis of the orientations of units A1 and A2, and may actually be several events. Bedding within unit A1 dips about 20°W, which is significantly different than its original subhorizontal easterly dip. In contrast, a soil developed in overlying unit A2 is subhorizontal, suggesting that the tilting of unit A1 preceded the deposition of unit A2. This backtilting of at least 20° likely is a result of several ruptures that occurred prior to about 140 ka (the minimum age estimated for unit A2, Fig. 8). We postulate that the closed depression within which unit A2 was deposited may be related to formation of a broad graben along the fault or to temporary damming of the Rendija Canyon drainage by a fault scarp.

Structural relations suggest the occurrence of a surface-faulting earthquake between deposition of units A2 and A3 (Earthquake W, Fig. 8). As noted above, unit A3 is not displaced by a subsidiary fault splay in trench GPT2 that exhibits prominent shearing within unit A2 (Fig. 7). In addition, there is little or no vertical separation of the base of the soil developed in unit A2. These relations suggest that at least one surface-faulting earthquake occurred prior to the period of soil formation on unit A2. Age constraints on the timing of this rupture event are poor, however, because the TL-based age estimate for unit A2 is a minimum (more than

about 140 ka; Table 1). A minimum-limiting age for Earthquake W is provided by an average TL age estimate of 65 ± 9 ka for unit C6, which is stratigraphically above unit A3 (Fig. 8).

The characteristics of units C5 and C6 provide evidence of a surface-rupture earthquake after deposition of alluvial unit A4 (Earthquake X, Fig. 8). This rupture produced a surface scarp from which both units C5 and C6 were derived. The proximal, debris-facies colluvium (unit C5) filled a 1-m-wide graben exposed in trench GPT1 (Fig. 6), and was locally deposited along the scarp face in the vicinity of trench GPT2 (Fig. 7). This deposit probably reflects spalling or raveling of the scarp face during or closely following Earthquake X. The wash-facies colluvium (unit C6) extends farther to the west and has an average TL age of 65 ± 9 ka. Earthquake X occurred prior to the deposition of basal unit C6, which could be as old as 74 ka. The lateral discontinuity and lack of soil development in unit C5 suggests that the deposition of the basal part of unit C6 probably occurred less than a thousand years after the rupture event, and thus the maximum age for Earthquake X is about 75 ka. A TL age estimate of 65 ± 9 ka for the basal part of unit C6 suggests that the youngest age for Earthquake X is 56 ka. However, the upper part of unit C6 contains soil development suggestive of several thousands of years of surface stability following Earthquake X. We believe the best estimate for the timing of Earthquake X is about 60 to 75 ka.

In order to consider all possible rupture scenarios, Wong et al. (unpubl. report for LANL, 1995) provide equivocal evidence of either one or two surface-rupture earthquakes since the deposition of unit C6. The older of these two events (Earthquake Y?, Fig. 8) was interpreted on the basis of apparent deformation of unit A4 adjacent to the fault. Near the fault, unit A4 appears to dip to the west, which is opposite to its inferred original subhorizontal easterly dip. Wong et al. (unpubl. report for LANL, 1995) also considered the possibility that the overlying unit C6 also may be tilted to the west away from the fault. Because the soil developed on unit C6 (Fig. 6) is subhorizontal and thus undeformed, we suggest that Earthquake Y? may have occurred on the RCF following the deposition of unit C6 but prior to the most-recent faulting event (Earthquake Z, Fig. 8). Although this scenario is possible, we believe that the evidence of tilting of unit C6 is weak, and that Earthquake Y? is suspect.

The most recent surface rupture at the Guaje Pines site (Earthquake Z, Fig. 8) displaced the lower package of scarp-derived colluvial deposits (units C5 and C6), and resulted in deposition of the upper scarp-derived colluvial deposits (units C7 and C8). The proximal, debris-facies colluvium (unit C7) was derived from unit A3 exposed in the scarp face, most likely shortly after the rupture event. The basal part of unit C7 in trench GPT1 filled a small depression or fissure along the base of the scarp. The wash-facies colluvium (unit C8) also was derived from the fault scarp. As noted above, the estimated age of the basal part of unit C7 is either 9 ka or 23 ± 4 ka. Thus, we interpret that Earthquake Z either occurred at about 9 ka, or at about 23 ka (Fig. 8).

In summary, subsurface investigations at the Guaje Pines site provide evidence of at least three and as many as five surface ruptures along the RCF (Fig. 8). The timing of the oldest rupture is known only to be older than 140 ± 26 ka. The three or four younger rupture events (Earthquakes W, X, Y?, and Z) occurred since deposition of unit A2, which is estimated to be more than 140 ± 26 ka. The timing of the Earthquake W is unknown. Earthquake X most likely occurred between about 60 and 75 ka, on the basis of age estimates of scarp-derived colluvium and soil development. If Earthquake Y? occurred, its timing is constrained between 8 and 75 ka. The most-recent rupture (Earthquake Z) occurred at about 9 ka or 23 ka, on the basis of age estimates from scarp-derived colluvium.

The occurrence of latest Pleistocene or possibly early Holocene activity along the RCF is comparable to paleoseismic information from the GMF, another component of the Pajarito fault system (Gardner et al., 1990). However, the most recent rupture along the GMF was about 4000 to 6000 yrs ago, which is younger than the most recent paleoearthquake on the RCF by at least 2000 yrs. The difference in timing between the most recent surface-faulting earthquakes on the RCF and GMF suggests that these faults may rupture independently from each other. In addition, the absence of conclusive evidence of Holocene or latest Pleistocene displacement from several paleoseismic trenches across the PAF suggests that the RCF and GMF also may rupture independently from the PAF. However, existing information on the timing of paleoearthquakes on the Pajarito fault system is inadequate to be conclusive about the interdependency of the RCF and the PAF (Olig et al., this volume).

### Displacement per earthquake

The amount of vertical separation produced by individual surface ruptures on a normal fault can be estimated based on models of scarp degradation (Nash, 1986; Forman et al., 1991; Nelson, 1992; McCalpin et al., 1993). Assuming the volume of material shed from the scarp equals that deposited on the downthrown side of the fault, the thickness of material deposited at the base of a fault scarp is approximately one-half of the original scarp height. Addition to or loss of material from the base of the scarp may yield estimates of vertical surface displacement that are too high or too low, respectively. In addition, backtilting and antithetic faulting may accentuate scarp height. At the Guaje Pines site, the preservation of the moderately developed soil in unit C8 suggests long-term surface stability, and little or no loss of the upper scarp-derived colluvium from trench GPT1. Because the alluvial surface at the Guaje Pines site slopes downstream, in the opposite direction as the scarp, the height of the fault scarp is a close approximation of the surface offset.

The thicknesses of units C7 and C8 in trench GPT1 provide a means to estimate the amount of displacement during the most recent earthquake (Fig. 6). These units together are 1.0 to 1.3 m thick west of the fault, suggesting that the scarp produced by Earthquake Z was about 2 to 2.6 m high. Considering that units C7 and C8 may include a component of loess, it is possible that the scarp was not quite as high, perhaps as small as 1.5 m. Thus, we interpret that the vertical displacement during the most-recent earthquake along the RCF is 2.0 ± 0.5 m. We cannot estimate the amount of displacement from earlier events because of subsequent erosion.

### Surface rupture recurrence

Our estimates of the timing of surface ruptures along the RCF provide a means to estimate the intervals between large earthquakes. Stratigraphic evidence of Earthquakes X and Z suggest that large earthquakes occur along the fault on the order of a few to several tens of thousands of years. Given our preferred estimate of about 60 to 75 ka for the timing of Earthquake X, and a range of 9 to 27 ka for the timing of Earthquake Z, we estimate that the amount of time between these ruptures is 33 to 66 ka. If Earthquake Y? also occurred, the average amount of time between events X, Y? and Z is one-half these values.

Average earthquake recurrence on longer geologic time scales ($10^5$ to $10^6$ years) can also be estimated using available data on long-term fault slip rate and displacement per event. The Guaje Pines site is located at or near the long-term maximum vertical displacement along the fault, which is 36 ± 10 m (Fig. 3; Olig et al., this volume). This value yields a long-term slip rate of 0.03 ± 0.01 mm/yr. On the basis of our trench data, the vertical displacement during the most recent surface-faulting event at the Guaje Pines site is estimated as 2.0 ± 0.5 m, as noted above. Using a slip rate of 0.03 ± 0.01 mm/yr and a displacement per event of 2.0 ± 0.5 m, the range in recurrence is 38 to 83 ky, with a preferred value of about 67 ky. These values compare favorably with the estimated recurrence intervals based on the timing of the two most recent paleoearthquakes at the site, and with intervals estimated for other major faults within the Rio Grande rift (Machette, 1987; Menges, 1990).

## CONCLUSIONS

The RCF is a integral part of the Pajarito fault system, which borders the active western margin of the Española Basin in the Rio Grande rift. Our paleoseismic trenches exposed older alluvium deposited by the east-flowing Rendija Canyon drainage, overlain by two packages of fining-upward colluvial deposits derived from the Rendija Canyon fault scarp. Each of the colluvial deposits contains a lower, discontinuous proximal debris facies close to the fault, and an upper, more extensive and finer-grained wash facies. Ages of the alluvial and colluvial deposits are estimated from radiocarbon and thermoluminescence analyses, and relative soil development. Both colluvial packages reflect degradation of scarps produced during surface-faulting earthquakes. Fault strands exposed in the trenches are moderately to steeply dipping, and have had west-down

normal displacement. The trench exposures provide evidence of at least three and possibly as many as five surface-faulting events, with the oldest of these occurring prior to about 140 ka. Three or four events occurred since deposition of alluvium that is more than 140 ± 26 ka. The most recent rupture occurred at about 9 ka or 23 ka, suggesting a latest Pleistocene or early Holocene surface-faulting event along the fault. The thickness of the upper colluvial package suggests a net vertical tectonic displacement during the most recent paleoearthquake of 2.0 ± 0.5 m. We estimate a preferred recurrence interval for surface-rupture earthquakes of between 31 and 66 ky on the basis of age estimates from scarp-derived colluvium, and an interval of about 38 to 83 ky on the basis of long-term slip rate and displacement per event data. The difference in timing between the most recent earthquakes on the RCF and GMF suggests that these faults may rupture independently from each other.

## ACKNOWLEDGMENTS

This study was supported by the U.S. Department of Energy (DOE) through the LANL Seismic Hazard Investigation Program, and was performed by Woodward-Clyde Federal Services (WCFS), William Lettis & Associates (WLA), and members of the Geology and Geochemistry Group of LANL. WCFS and WLA personnel were supported by LANL Contract 9-XT1-092K-1. Sincere appreciation for collection of field data and lively discussion goes to Karen Carter, Scott Baldridge, and John Carney of LANL, Norma Biggar, Jackie Bott, Jim Springer, and Janet Sawyer of WCFS, and Bill Lettis, Jay Noller, and Colleen Haraden of WLA. Special gratitude to Dean Keller and Doug Volkman of LANL, and Jeff Kimball of DOE for their support of our efforts. Technical reviews of this study were provided by Michael Machette of the USGS, Jim McCalpin of GEO-HAZ Consultants, Al Sanford of New Mexico Tech, and Mike Cline of WCFS. Mike Machette and Bill Lettis graciously provided technical review of this paper on short notice.

## REFERENCES

Carter, K. E. and Gardner, J. N., 1995, Quaternary fault kinematics in the northwestern Española Basin, Rio Grande rift, New Mexico: New Mexico Geological Society, Guidebook 46, p. 97–103.

Forman, S. L., Nelson, A. R. and McCalpin, J. P., 1991, Thermoluminescence dating of fault-scarp-derived colluvium: deciphering the timing of paleoearthquakes on the Weber segment of the Wasatch fault zone, north central Utah: Journal of Geophysical Research, v. 96, p. 595–605.

Gardner, J. N., Baldridge, W. S., Gribble, R., Manley, K., Tanaka, K., Geissman, J. W., Gonzalez, M. and Baron, G., 1990, Results from seismic hazards trench #1 (SHT-1), Los Alamos seismic hazards investigations: Los Alamos National Laboratory, Report EES1-SH90-19, 57 p.

Gardner, J. N. and House, L., 1987, Seismic hazards investigations at Los Alamos National Laboratory, 1984-1985: Los Alamos National Laboratory Report, LA-11072-MS, 76 p.

Kelson, K. I. and Olig, S. S., 1995, Estimated rates of Quaternary crustal extension in the Rio Grande rift, northern New Mexico: New Mexico Geological Society, Guidebook 46, p. 9–12.

Machette, M. N., 1987, Preliminary assessment of Quaternary faulting near Truth or Consequences, New Mexico: U.S. Geological Survey, Open-file Report 87–652, 39 p.

McCalpin, J. P., Zuchiewicz, W. and Jones, L. C. A., 1993, Sedimentology of fault-scarp-derived colluvium from the 1983 Borah Peak rupture, central Idaho: Journal of Sedimentary Petrology, v. 63, p. 120–130.

McDonald, E. V., Reneau, S. L. and Gardner, J. N., 1996, Soil-forming processes on the Pajarito Plateau: investigation of a soil chronosequence in Rendija Canyon: New Mexico Geological Society, Guidebook 47.

Menges, C. M., 1990, Late Quaternary fault scarps, mountain-front landforms, and Pliocene-Quaternary segmentation on the range-bounding fault zone, Sangre de Cristo Mountains, New Mexico; *in* Krinitsky, E. L. and Slemmons, D. B., eds., Neotectonics in earthquake evaluation: Geological Society of America Reviews in Engineering Geology, v. 8, p. 131–156.

Nash, D. B., 1986, Morphologic dating and modeling degradation of fault scarps; *in* Active tectonics—studies in geophysics: Washington, D.C., National Academy Press, p. 181–194.

Nelson, A. R., 1992, Lithofacies analysis of colluvial sediments—an aid in interpreting the recent history of Quaternary normal faults in the Basin and Range province, western U.S.: Journal of Sedimentary Petrology, v. 62, p. 607–621.

Olig, S. S., Kelson, K. I., Gardner, J. N. and Reneau, S., 1996, The earthquake potential of the Pajarito fault system: New Mexico Geological Society, Guidebook 47.

Smith, R. L., Bailey, R. A., and Ross, C. S., 1970, Geologic map of the Jemez Mountains, New Mexico: U.S. Geological Survey, Miscellaneous Investigations Map I-571, scale 1:125,000.

Stuiver, M. and Reimer, P. J., 1993, Extended $^{14}C$ data base and revised CALIB 3.0 $^{14}C$ age calibration: Radiocarbon, v. 35, p. 215–230.

Wong, I., Kelson, K., Olig, S., Bott, J., Green, R., Kolbe, T., Hemphill-Haley, M., Gardner, J., Reneau, S. and Silva, W., 1996, Earthquake potential and hazards at Los Alamos National Laboratory, New Mexico: New Mexico Geological Society, Guidebook 47.